


















RESEARCH ARTICLE

Electrolyte-gated organic field-effect transistors with high operational stability and lifetime in practical electrolytes

Dimitrios Simatos^{1,2}  | Mark Nikolka¹  | Jérôme Charmet^{3,4}  |
 Leszek J. Spalek¹  | Zenon Toprakcioglu²  | Ian E. Jacobs¹  |
 Ivan B. Dimov⁵  | Guillaume Schweicher⁶  | Mi Jung Lee⁷  |
 Carmen M. Fernández-Posada⁸  | Duncan J. Howe²  | Tuuli A. Hakala²  |
 Lianne W. Y. Roode² | Vincenzo Pecunia⁹  | Thomas P. Sharp¹ |
 Weimin Zhang¹⁰ | Maryam Alsufyani¹¹  | Iain McCulloch^{10,11}  |
 Tuomas P. J. Knowles²  | Henning Sirringhaus¹ 

¹Optoelectronics Group, Cavendish Laboratory, University of Cambridge, Cambridge, UK

²Yusuf Hamied Department of Chemistry, University of Cambridge, Cambridge, UK

³School of Engineering—HE-Arc Ingénierie, HES-SO University of Applied Sciences Western Switzerland, Neuchâtel, Switzerland

⁴Faculty of Medicine, University of Bern, Bern, Switzerland

⁵Electrical Engineering Division, Department of Engineering, University of Cambridge, Cambridge, UK

⁶Laboratoire de Chimie des Polymères, Faculté des Sciences, Université Libre de Bruxelles (ULB), Bruxelles, Belgium

⁷School of Natural Science, Taejæ University, Seoul, Republic of Korea

⁸Maxwell Centre, Department of Physics, Cambridge, UK

⁹School of Sustainable Energy Engineering, Faculty of Applied Sciences, Simon Fraser University, Surrey, British Columbia, Canada

¹⁰Physical Science and Engineering Division, King Abdullah University of Science and Technology (KAUST), Thuwal, Saudi Arabia

¹¹Department of Chemistry, University of Oxford, Oxford, UK

Correspondence

Mark Nikolka and Henning Sirringhaus,
 Optoelectronics Group, Cavendish
 Laboratory, University of Cambridge, J.J.
 Thomson Ave, Cambridge CB3 0HE, UK.
 Email: mn390@cam.ac.uk and
hs220@cam.ac.uk

Tuomas P. J. Knowles, Yusuf Hamied
 Department of Chemistry, University of
 Cambridge, Lensfield Rd, Cambridge CB2
 1EW, UK.
 Email: tpjk2@cam.ac.uk

Jérôme Charmet, School of Engineering
 —HE-Arc Ingénierie, HES-SO University
 of Applied Sciences Western Switzerland,
 2000 Neuchâtel, Switzerland.
 Email: jerome.charmet@he-arc.ch

Abstract

A key component of organic bioelectronics is electrolyte-gated organic field-effect transistors (EG-OFETs), which have recently been used as sensors to demonstrate label-free, single-molecule detection. However, these devices exhibit limited stability when operated in direct contact with aqueous electrolytes. Ultrahigh stability is demonstrated to be achievable through the utilization of a systematic multifactorial approach in this study. EG-OFETs with operational stability and lifetime several orders of magnitude higher than the state of the art have been fabricated by carefully controlling a set of intricate stability-limiting factors, including contamination and corrosion. The indacenodithiophene-co-benzothiadiazole (IDTBT) EG-OFETs exhibit operational stability that exceeds 900 min in a variety of widely used electrolytes, with an overall lifetime exceeding 2 months in ultrapure water and 1 month in

This is an open access article under the terms of the [Creative Commons Attribution](https://creativecommons.org/licenses/by/4.0/) License, which permits use, distribution and reproduction in any medium, provided the original work is properly cited.

© 2024 The Authors. *SmartMat* published by Tianjin University and John Wiley & Sons Australia, Ltd.

Funding information

Engineering and Physical Sciences Research Council (EPSRC), Grant/Award Numbers: EP/R031894/1, EP/R032025/1, EP/W017091/1; EPSRC Centre for Doctoral Training (CDT), Grant/Award Number: EP/L015889/1; EPSRC Cambridge NanoDTC, Grant/Award Number: EP/L015978/1; Belgian National Fund for Scientific Research (FNRS) COHERENCE2, Grant/Award Number: F.4536.23; Francqui Foundation Francqui Start-Up Grant; Royal Society Research Professorship, Grant/Award Number: RP/R1/201082; Henry Royce Institute facilities, Grant/Award Number: EP/P024947/1; Henry Royce Institute recurrent, Grant/Award Number: EP/R00661X/1

various electrolytes. The devices were not affected by electrical stress-induced trap states and can remain stable even in voltage ranges where electrochemical doping occurs. To validate the applicability of our stabilized device for biosensing applications, the reliable detection of the protein lysozyme in ultrapure water and in a physiological sodium phosphate buffer solution for 1500 min was demonstrated. The results show that polymer-based EG-OFETs are a viable architecture not only for short-term but also for long-term biosensing applications.

KEYWORDS

contaminants, galvanic corrosion, long-term sensing, organic electronics, organic field-effect transistors, water stability

1 | INTRODUCTION

Electrolyte-gated organic field-effect transistors (EG-OFETs) are a variation of the regular, three-terminal organic field-effect transistor (OFET) architecture in which an aqueous electrolyte replaces the solid-state dielectric (Figure 1A).¹ When the gate electrode of an EG-OFET is biased e.g., negatively, a layer of electrolyte cations is electrostatically attracted towards the metal/electrolyte interface, forming a layer and partially screening the electric field. The two layers of charges in the metal and the electrolyte form an electrical double layer (EDL). Similarly, a layer of anions is repulsed towards the electrolyte/semiconductor interface, and attracts a layer of charge carriers in the semiconductor side. Hence, two Å-thick EDLs form, with one being at the gate/electrolyte and the other at the electrolyte/semiconductor interface. In electrolytes with low ionic strength, such as ultrapure water, the two EDLs form over much longer timescales and multiple measurement cycles. Each layer has a capacitance on the order of $\mu\text{F}/\text{cm}^2$,² which allows for low-voltage (<1 V) transistor operation.³ This feature, combined with their intrinsic sensitivity, makes EG-OFETs ideal candidates for biosensing applications. In the context of biosensing, the detection of target molecules is often done in real time using consecutive measurements and, depending on the application, the measurements may last between minutes to days.⁴⁻⁷ This necessitates the development of biosensors with long-term operational stability in a variety of electrolytes. While EG-OFETs have recently achieved label-free, single-molecule detection,⁸ they exhibit

limited operational stability, similarly to other organic electronic devices that are operated in direct contact with aqueous electrolytes. A typical manifestation of this instability is a significant current drift (i.e., increase or decrease) over time.⁹⁻¹⁴ The physical mechanisms that cause this instability are not clearly understood. It is believed that one of the mechanisms is the formation of water-induced traps when water molecules diffuse into a semiconducting polymer. These traps are generated due to the high dipole moment of water molecules, which introduces torsional and other defects in the polymer backbone, as well as dipole-induced energetic disorder.¹⁵ Electrolytes with larger ionic strength, such as biosensing-relevant saline solutions or buffers, introduce even more pronounced instabilities.¹⁰

There are additional physical mechanisms that cause EG-OFETs to degrade in aqueous media, which are not yet fully understood. It is known that the operating voltages (i.e., gate voltage: V_G , drain voltage: V_D) of EG-OFETs play a critical role in their stability performance. Exceeding a so-called “stable operational window” results in electrochemical reactions that rapidly decrease the ON current and irreversibly degrade the device, even if the operating voltages are reduced again.^{10,14,16-18} This is attributed to the electrochemical doping (oxidation) of the organic semiconductor.^{17,18} It is believed that the high voltages cause ions to penetrate deeper in the semiconductor thin film,^{19,20} which changes the surface wettability^{21,22} and leads to changes in the dimensionality of charge transport.^{23,24} The signature of this irreversible degradation is a Faradaic leakage current (i.e., from the gate electrode to the semiconductor) that

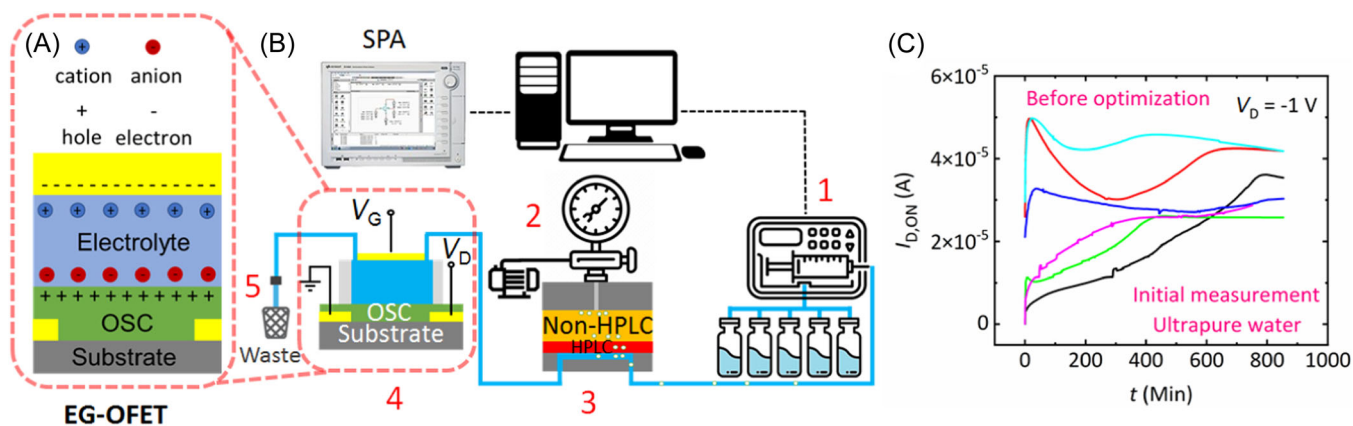


FIGURE 1 The device structure, the experimental setup, and the operational stability challenges of indacenodithiophene-co-benzothiadiazole (IDTBT) electrolyte-gated organic field-effect transistors (EG-OFETs). (A) The structure of an EG-OFET. (B) Schematic diagram of the experimental setup used to measure EG-OFETs. It consists of (1) a syringe pump that can draw liquid from multiple reservoirs and pump it sequentially through (2) a vacuum regulator-controlled (3) bubble trap, the (4) EG-OFET, and the (5) waste container. A semiconductor parameter analyzer (SPA) was used for the electrical measurements. In the bubble trap, an additional high-performance liquid chromatography grade (HPLC-grade) polytetrafluoroethylene (PTFE) membrane is placed on top of the original (non-HPLC-grade) one, to interface with the liquid and avoid leaching contaminants that affect the device stability. (C) The ON current evolution during the initial operational stability experiment for different batches of IDTBT EG-OFETs in ultrapure water. Each curve corresponds to the initial overnight experiment using a freshly fabricated device. A transfer curve per minute was acquired ($V_{G,max} = V_D = -1$ V), and the absolute value of the ON current (I_D for $V_G = -1$ V) was plotted as a function of time. Large operational stability variations are observed despite the fact that the EG-OFETs were fabricated under nominally identical conditions.

increases with consecutive device measurements.^{16,17} Moreover, the stable operational window is limited by the hydrolysis limit of -1.23 V (vs. standard hydrogen electrode—SHE).²⁵ Hence, the overall potential difference between electrodes in a field-effect transistor (FET) cannot exceed 1.23 V, without detrimental H_2 and O_2 production.

Other components might affect the oxidation and reduction potentials and further reduce the EG-OFET's stable operational window. These include the semiconductor material²⁶ and/or any additives incorporated therein,^{15,27} as well as the type and/or the ionic strength of the electrolyte.¹⁰ In device studies, the electrochemical potential at which degradation sets in due to a specific electrochemical process is often not of so much of interest and therefore typically not reported. Even when these values are reported, there is still some uncertainty due to the mismatch between an FET and a redox cell. FET operating voltages are referenced versus the grounded source electrode (source voltage: $V_S = 0$ V), whereas in electrochemistry conventions, the potentials are reported versus a reference electrode (e.g., SHE, Ag/AgCl). Since an FET is a two-terminal cell with the gate being both a working and reference electrode, the absolute potential in the electrolyte is not exactly defined, even at $V_G = 0$. Hence, the maximum potential difference that can be applied (the stable operational window) is more relevant for device operation. Poly-3-

hexylthiophene (P3HT) EG-OFETs were reported to have an operational window of 0.6 V (i.e., $V_{G,max} = -0.6$ V) in deionized (DI) water^{16,17} and phosphate buffer saline ($1 \times$ PBS).¹⁸ However, a follow-up study determined the stable operational window to be 0.3 V.²⁸ In most cases, the EG-OFET's stable operational window is determined empirically, by choosing the operating voltages that minimize the leakage current.⁸

Surprisingly, there are only a few long-term operational stability studies of EG-OFETs in the literature.^{12,14,29} The first long-term study was performed on EG-OFETs made from small molecule organic semiconductors.¹² The ON current of those devices in ultrapure water decreased by 35% – 40% in the first 11 h ($3\%/h$), while their lifetime was not reported. The devices also remained operational in NaCl 1 mol/L but only in operating voltages where electrochemical doping did not occur. Regarding EG-OFETs made from semiconducting polymers, Picca et al.¹⁴ showed that the degradation of P3HT EG-OFETs in ultrapure water can be split into two regimes: an initial stabilization regime, which lasts for the first 24 h, followed by a second regime during the following period of several weeks. In the initial regime, the ON current of a freshly fabricated device decreases within the first few measurements and eventually reaches a steady state within 24 h. This degradation was attributed to the diffusion of water between the polymer chains and the subsequent

generation of water-induced traps. The second regime is a much slower degradation regime, where the ON current decreases slowly with time (1%/h), due to the threshold voltage shifting to more negative values. The ON current of those devices decreased by 35% in the first 24 h and by 60% in 15 days, while their lifetime did not exceed 20 days. It is worth mentioning that a similar two-regime degradation has been observed in electrolyte-gated FETs made from inorganic semiconductors.³⁰ A follow-up study on identical devices by Luukkonen et al.²⁹ split the water degradation into two concurrent regimes: a short-term regime, which manifests as a threshold voltage shift during the first measurements of each experiment (i.e., regardless if the device is fresh or not), and a long-term regime that spans across the entire lifetime of the device. In the short-term regime, the threshold voltage shifts closer to zero. This effect was attributed to changes in the work function of the gate electrode and does not appear if the gate electrode remains submerged in water between experiments. In the long-term regime, the ON current decreases linearly with the number of measurements, and the degradation rate depends on how frequently the device is measured. This degradation was attributed to an increase in the density of electrical stress-induced trap states, which manifests as a threshold voltage shift and a decrease in mobility. This degradation mechanism contradicts the findings of the earlier study. First of all, the new study suggests that the device only degrades when it is measured in water and not when it is simply immersed in it. In other words, the degradation mechanism is electrochemical, with the device degrading even when it is measured within the stable operational window. Second, the ON current drift of 1%/h that was mentioned in the earlier study only occurs if the interval between measurements is 30 min. If this interval is reduced to 30 s, the degradation is much larger, and the device is unable to reach a steady state. In the new study, the ON current decreased by 67% in 5750 measurement cycles, while the device lifetime was not reported. Both of these studies were done in ultrapure water, while electrolytes with larger ionic strength, such as biosensing-relevant saline solutions or buffers, were not examined.

In this work, we present EG-OFET devices with ultrahigh operational stability and lifetime, suitable for long-term biosensing applications in aqueous electrolytes. This was achieved using a systematic approach to fine-tune individual process steps and eliminate multiple degradation factors. The devices presented in this study are based on indacenodithiophene-co-benzothiadiazole (IDTBT), a high-mobility polymer widely studied for OFET applications,^{31–34} which has demonstrated fast turn-on and an improved subthreshold swing when used

in EG-OFETs.³⁵ We identified galvanic corrosion and leachable contaminants as two major mechanisms that cause device degradation in water. After overcoming these issues, the stabilized EG-OFETs remain stable for an overnight experiment (≈ 900 min) in a variety of electrolytes (ultrapure water, saline solution, $1 \times$ PBS buffer, sodium phosphate (NaP) buffer). We explain the different requirements to achieve stability in each of these electrolytes. Our devices have a median current drift of $\approx 0.2\%/h$ in ultrapure water, $\approx 0.1\%/h$ in $1 \times$ PBS, and $<0.1\%/h$ in saline solution and NaP buffer. The overall device lifetime exceeds 2 months in ultrapure water and 1 month in the other electrolytes. The devices were not affected by electrical stress-induced trap states and can remain stable even in voltage ranges where electrochemical doping occurs. To validate the applicability of our stabilized device for biosensing applications, we performed experiments using the protein lysozyme as a model biomolecule.³⁶ We show that the stabilized EG-OFETs are able to sense lysozyme in ultrapure water and NaP buffer, with the baseline (ON current evolution over time) remaining stable during injections of the same solution, while the sensing response scales with the lysozyme concentration. The operational stability and lifetime of our IDTBT EG-OFETs in aqueous electrolytes exceed the corresponding metrics of other devices reported in the literature to date.

2 | METHOD

Conducting long-term operational stability experiments in a liquid poses several experimental challenges. Electrochemical reactions may take place,^{10,14,16–18} the metal contacts may degrade,^{37–39} and contaminants (impurities, leachables, and extractables) may degrade the device during the measurement.^{40–48} Air bubbles may also disrupt the experiment if the device is integrated with microfluidic channels.⁴⁹ All operational stability studies on EG-OFETs published to date have been conducted in “static mode”, that is, with a polymer well, typically polydimethylsiloxane (PDMS), confining a volume of liquid above the active area.^{12,14,29} This configuration does not allow for continuous liquid injections inside the device (dynamic mode). This means that any byproducts of potential electrochemical reactions occurring during the degradation process remain and accumulate in the flow cell. Moreover, static mode biosensing is unfavorable in many real-life situations, due to the device operating in a diffusion-limited regime, which results in the formation of a depletion zone that limits the analyte collection efficiency.⁵⁰

To measure the EG-OFET in dynamic mode, an experimental setup was designed to perform automated, long-term microfluidic experiments without the interference of air bubbles. The setup can inject liquids through the flow cell, while tracking the EG-OFET's performance metrics (ON current, OFF current) over time. Figure 1B shows the diagram of the experimental setup, and a detailed description can be found in the "Experimental setup" section of Supporting Information (Supporting Information S1: Figures S1, S2). The setup consists of a syringe pump that can draw liquid from multiple reservoirs and pump it sequentially through a vacuum regulator-controlled bubble trap, the EG-OFET, and the waste container. The liquid was injected within a span of 8 min, and then the device was allowed to stabilize for at least 30 min before the next liquid injection occurred (see "Experimental parameters" section of Supporting Information). During the entire experiment, the device was measured constantly, at a rate of one transfer curve per minute. A semiconductor parameter analyzer (SPA) was used for the electrical measurements. The mitigation of air bubbles is described in detail in the "Air bubbles" section of Supporting Information (Supporting Information S1: Figures S3, S4, S5, S6, S7). In brief, we used a bubble trap in which an additional high-performance liquid chromatography grade (HPLC-grade) polytetrafluoroethylene (PTFE) membrane is placed on top of the original (non-HPLC-grade) one to interface with the liquid and avoid leaching contaminants that affect the device stability. The EG-OFET itself consists of the IDTBT-coated bottom source-drain contacts on a glass substrate, with a PDMS flow cell and a 0.1 mm-thick Pt sheet as the gate electrode. A poly(methyl methacrylate) (PMMA) clamp compresses the entire device and ensures its water tightness. A more detailed description of the device architectures used in this study can be found in the "Device architecture" section of Supporting Information (Supporting Information S1: Figures S8, S9).

3 | EXPERIMENT RESULTS

3.1 | Factors affecting EG-OFET operational stability

We first conducted an initial screening of the operational stability of our first generation of IDTBT EG-OFETs in ultrapure water. A detailed description of the fabrication and experimental details of the different device generations can be found in the "Experimental methods" section of Supporting Information. Figure 1C shows operational stability (ON current evolution over time) measurements in ultrapure water of nominally identical

devices fabricated in different batches. Each curve corresponds to the initial overnight experiment using a freshly fabricated device. A transfer curve per minute was acquired ($V_{G,max} = V_D = -1$ V), and the absolute value of the ON current (I_D for $V_G = -1$ V) was plotted as a function of time (see "Experimental methods" section in Supporting Information). There were substantial operational stability variations between the devices, and none of the devices reached a steady state at the end of the first overnight experiment, unlike our optimized devices presented below. This motivated us to conduct a systematic study to trace the origins of these variations and improve EG-OFET stability.

The first degradation factor that we identified was contamination originating from the N_2 glovebox and plastic laboratory consumables widely used during film processing as well as liquid handling (disposable needles, plastic pipettes, syringes, and centrifuge tubes). Due to the complexity inherent to the identification of the many sources of contamination, we have conducted a separate study, using solution nuclear magnetic resonance (NMR) spectroscopy as a technique to identify the molecular structure of the contaminants and trace their origin.⁴⁰ This study identified the effects of contamination on device performance, water uptake, and thin-film properties and also enabled us to define the optimal processing conditions reported herein. Figure 2 summarizes the effect of contaminants originating from plastic laboratory consumables and from contaminants in the PDMS on EG-OFET stability. Figure 2A shows the operational stability of an IDTBT EG-OFET in NaP buffer. The spikes in the ON current (red curve) coincide with the liquid injections from the syringe pump (orange curve). The device is initially able to maintain a stable baseline in NaP buffer. However, injecting NaP buffer preheated in plastic centrifuge "Falcon" tubes (37°C/24 h) causes the ON current to decrease. The device did not recover when injected with fresh NaP buffer. The same baseline decrease was observed when the device was injected with NaP buffer in which we washed plastic pipettes (20 pipettes, 10× each/5 mL) and plastic syringes (10 syringes, 1× each/5 mL). This suggests that contaminants leaching from plastic laboratory consumables can affect the EG-OFET baseline and create a response that resembles a sensing event. It will be shown later (see Figure 4) that our optimized devices remain stable during an individual overnight experiment (≈900 min), with consecutive liquid injections not affecting the ON current's slope and magnitude.

Another contaminant that was found to affect EG-OFET stability is residual un-crosslinked PDMS. Figure 2B shows EG-OFETs measured in ultrapure water using old (black curve) and new (red curve) PDMS flow

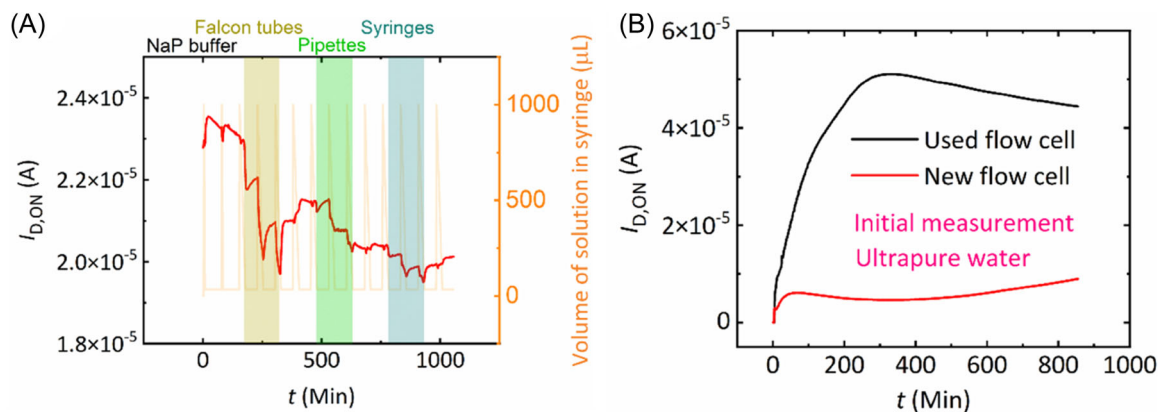


FIGURE 2 The effect of contaminants on electrolyte-gated organic field-effect transistor (EG-OFET) stability. (A) Operational stability of indacenodithiophene-co-benzothiadiazole (IDTBT) EG-OFETs in sodium phosphate (NaP) buffer. The vertical triangular spikes correspond to the liquid injections (orange curve). The ON current baseline (red curve) is affected by contaminants leaching from plastic centrifuge “Falcon” tubes, plastic pipettes, and plastic syringes. (B) Comparison of EG-OFETs in ultrapure water, measured with used (black curve), and new (red curve) polydimethylsiloxane (PDMS) flow cells. The degraded performance of the device measured with the new PDMS flow cell was attributed to residual un-crosslinked PDMS, which leaches from newly fabricated PDMS chips. Immersion of the PDMS flow cell in ultrapure water for a day is sufficient to remove the un-crosslinked PDMS.

cells. Each curve corresponds to the initial overnight experiment using a freshly fabricated device. The old flow cell, used in multiple experiments ($n > 10$), had been effectively washed with ultrapure water at least five times per experiment. The new PDMS flow cell had been used directly after fabrication, without a post-fabrication washing step. The degraded performance and lower stabilized ON current of the device measured with the new PDMS flow cell were attributed to residual un-crosslinked PDMS, which is known to leach from newly fabricated microfluidics and affect performance.⁵¹ We empirically observed that immersing the freshly fabricated PDMS flow cells in DI water for a day constitutes the simplest yet very effective cleaning protocol.

Another source of EG-OFET degradation, which became apparent when we performed stability studies in saline solution, was identified as galvanic corrosion of the metal contacts. This phenomenon can occur whenever two metals of different electrode potentials are biased and exposed to a conductive electrolyte, thus forming an electrochemical cell. A “galvanic” current then flows from the less noble metal (anode) to the noble one (cathode), resulting in corrosion of the anode and metal migration damage.⁵² OFET/EG-OFET contacts are typically made of Au with Cr or Ti adhesion layers to glass substrates, but these corrode when the underlying adhesion layer becomes exposed to the electrolyte through pinholes in the Au layer.³⁸ The adhesion layer of an individual electrode then acts as the anode and its overlying Au layer as the cathode. In chloride-containing electrolytes, Au is oxidized to form soluble AuCl^- complexes.⁵³ The electrochemical reaction results

in the partial delamination of the Au film and the formation of characteristic dome-like patterns.³⁸ Ti/Pt/Au emerged as a corrosion-resistant contact,³⁸ with further studies showing that Pt catalyzes the oxidation of Ti to TiO_2 ,⁵⁴ which acts as a passivation barrier.⁵⁵

Figure 3 shows the effect of galvanic corrosion on EG-OFET stability. Figure 3A shows initial day operational stability measurements of IDTBT EG-OFETs in saline solution. The corresponding OFF currents are shown in Supporting Information S1: Figure S10. EG-OFETs with Cr/Au (black curve) and Ti/Au (red curve) source-drain contacts exhibited a rapidly decreasing ON current, whereas those with Ti/Pt/Au contacts (green curve) had a baseline that eventually reached a steady state at the end of the first overnight experiment. EG-OFETs with a Cr adhesion layer degraded much faster than those with Ti. Figure 3B compares optical microscopy images of the source contacts of the three different EG-OFETs, imaged after the end of the experiment. In line with the stability measurements, Cr/Au contacts were the most corroded, with the Au layer being almost fully delaminated. Ti/Au contacts suffered from the characteristic dome-like corrosion patterns that are reported in the literature,³⁸ and Ti/Pt/Au contacts remained intact. We believe that Ti/Au contacts are more corrosion-resistant than Cr/Au because Ti and Au form two distinct layers, which means that Au encapsulates the Ti layer to a degree. In contrast, Cr interdiffuses with Au, forming an alloy.⁵⁶ We systematically studied the effect of the thickness of the Ti adhesion layer—and the formation of a TiO_2 passivation layer within the metal stack—on the stability of EG-OFETs made with Ti/Pt/Au contacts (Supporting Information S1: Figure S11).

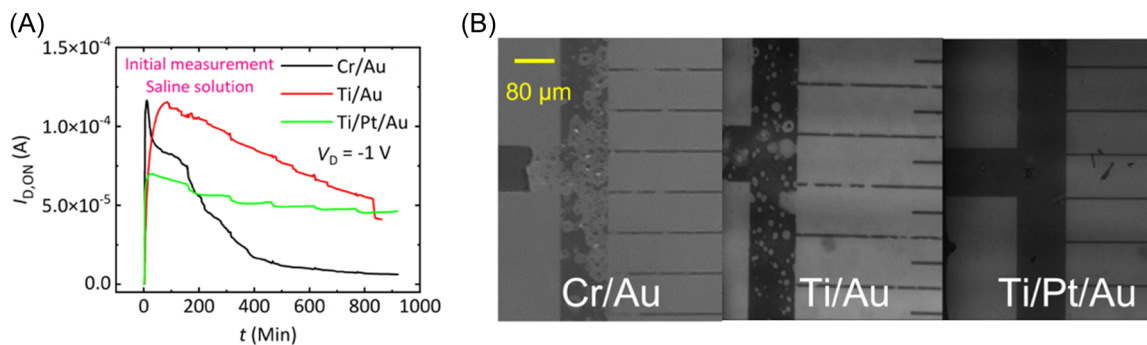


FIGURE 3 The effect of galvanic corrosion on electrolyte-gated organic field-effect transistor (EG-OFET) stability. (A) Initial day operational stability measurements of indacenodithiophene-co-benzothiadiazole (IDTBT) EG-OFETs in saline solution. EG-OFETs with Cr/Au (black curve) and Ti/Au (red curve) source-drain contacts exhibited a rapidly decreasing ON current, whereas those with Ti/Pt/Au contacts (green curve) had a baseline that eventually reached a steady state at the end of the first overnight experiment. (B) The source contacts of the three different EG-OFETs imaged after the end of the experiment. In line with the stability measurements, Cr/Au contacts looked to be the most corroded, with the Au layer being almost fully delaminated. Ti/Au contacts exhibited circular dome-like corrosion patterns, and Ti/Pt/Au contacts remained intact. Only the (grounded) source electrode corrodes, whereas the (negatively biased) drain electrode does not.

Galvanic corrosion depends on many factors, such as the potential difference between the anode and the cathode, the conductivity of the electrolyte, the electrode surface conditions, and the electrode areas.⁵² Indeed, galvanic corrosion on Ti/Au electrodes was suppressed when measuring in ultrapure water, when reducing the operating voltages to -0.6 V, and when increasing the thickness of the IDTBT film by using a denser IDTBT solution (Supporting Information S1: Figure S12). This suppression will not be observed for degradation that originates from exceeding the stable operational window of the organic semiconductor. In that case, the ON current was found to keep decreasing even when the operating voltages were reduced again.^{10,14,16–18} Hence, the operating voltage limits imposed due to galvanic corrosion are different from those imposed due to the oxidation and reduction of the organic semiconductor. Galvanic corrosion is also different from the oxygen-mediated degradation mechanism observed in p-type thiophene-based organic electrochemical transistors (OECTs).⁵⁷ Both degradation mechanisms are enhanced by the presence of dissolved oxygen in the electrolyte. However, corrosion results from the oxidation of the (grounded) source electrode, whereas the degradation mechanism observed in thiophene-based OECTs results from the reductive bias stress at the (negatively biased) drain electrode.

3.2 | Performance of optimized IDTBT EG-OFETs

Figure 4 presents the operational stability of optimized IDTBT EG-OFETs in ultrapure water, saline solution, $1 \times$ PBS, and NaP buffer, measured over a period of several

weeks. Each curve corresponds to a 900-min overnight experiment. Between experiments, the EG-OFET was stored while keeping the active area constantly hydrated (see “Disassembling and storing the device” section in Supporting Information), as in the literature.^{11,14,29} The corresponding OFF currents and transfer curves are shown in Supporting Information S1: Figures S13 and S14, respectively. For the optimized devices in Figure 4, we used Ti/Pt/Au source-drain contacts and avoided contamination from plastic tubes, syringes, pipettes, and the PDMS flow cells. We found the operational stability of these devices to be much more reproducible from batch to batch compared with the nonoptimized devices in Figure 1C. The operational stability was also similar across all electrolytes and matches the two-regime degradation reported in the literature for electrolyte-gated FETs.^{14,30} We distinguish between an initial stabilization “regime I”, which lasts for the first 900-min overnight experiment using a freshly fabricated device (i.e., the black curve in all four subfigures), followed by a “regime II” during the following period of several weeks. In regime I, the ON current of a freshly fabricated device initially overshoots to a high value, then rapidly decreases within the first few measurements, and eventually reaches a steady state at the end of the first overnight experiment. Regime II is a much slower degradation regime, where the ON current slowly increases with time at the start of the experiment, reaches a steady state, and then remains stable for the duration of a 900-min overnight experiment, with the baseline decreasing slowly from day to day.

In regime I, the ON current evolution can be split into three stages: an initial overshoot, followed by a rapid (approximately exponential¹⁴) decrease, and a

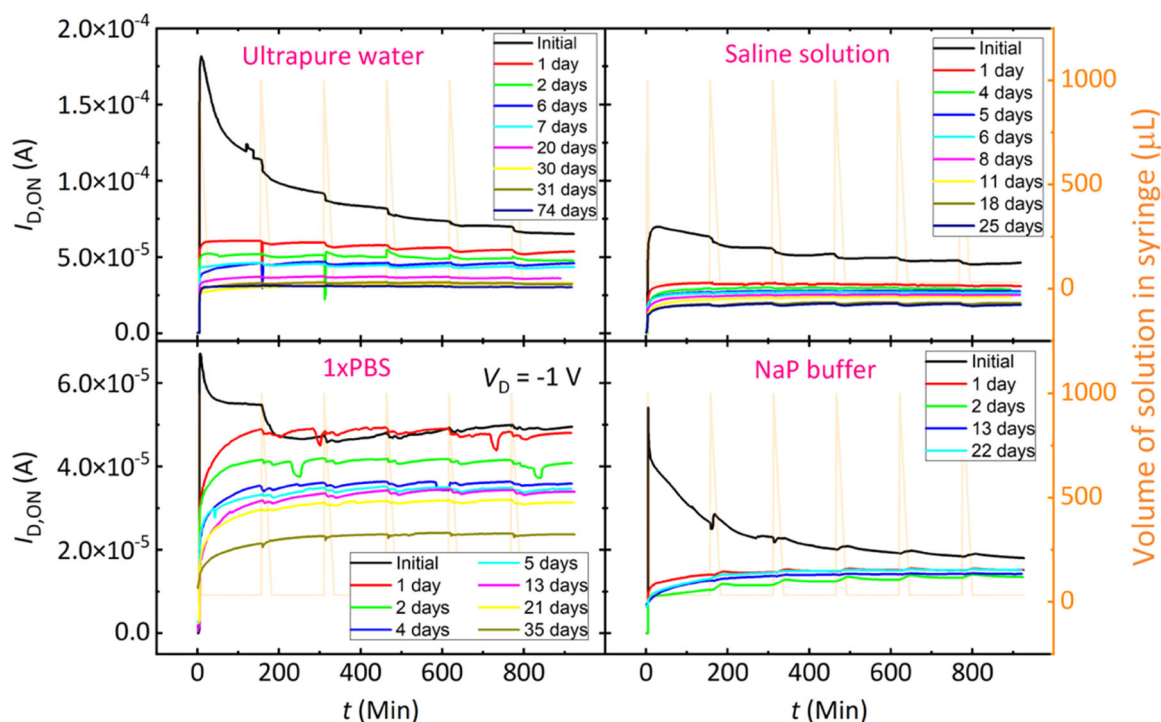


FIGURE 4 Operational stability of optimized indacenodithiophene-co-benzothiadiazole (IDTBT) electrolyte-gated organic field-effect transistors (EG-OFETs) in ultrapure water, saline solution, $1 \times$ PBS, and sodium phosphate (NaP) buffer, measured over a period of several weeks. Each curve corresponds to a 900-min overnight experiment. The vertical triangular spikes correspond to the liquid injections (orange curve). The degradation of IDTBT EG-OFETs in all four electrolytes can be split into two regimes: an initial “regime I”, where the ON current of a freshly fabricated device initially overshoots to a high value, then rapidly decreases within the first few measurements, and eventually reaches a steady state at the end of the first overnight experiment, followed by a much slower degradation “regime II”, where the ON current can remain stable for the duration of a 900-min overnight experiment, with the baseline decreasing slowly from day to day.

stabilization stage. In this regime, the ON current also decreases stepwise every time fresh liquid is injected. The overshoot occurs within the first 30 min, usually after the first liquid injection is finished (≈ 8 th min). It also appears regardless of the type of bottom contacts used (Figure 3A), although devices made using corrosion-resistant Ti/Pt/Au contacts have a smaller overshoot than devices made using Cr/Au or Ti/Au contacts that corrode. This overshoot has been previously observed in other long-term operational stability studies of EG-OFETs.^{12,29} However, the stepwise decrease of the ON current has not been reported so far, probably because EG-OFETs are typically measured in static mode.^{14,29} As mentioned in the introduction, the ON current decrease of P3HT EG-OFETs in regime I has been attributed to water-induced traps.¹⁴ In our study, regime I was observed on most of the devices, but there were some devices in which it was not observed (Supporting Information S1: Figure S15). Thus, it is unlikely to originate only from water-induced traps. We know that regime I is affected by any contamination present in the device. The ON current of the optimized devices was able to reach a steady state at the end of the first overnight

experiment, unlike the nonoptimized devices reported in Figure 1C. Reducing the operating voltages from -1 V to -0.6 V was found to suppress regime I, which suggests that it may be an electrochemical effect. In this case, the device operates only in regime II: in every overnight experiment (including the first one), the ON current slowly increases, reaches a steady state, and then remains stable for the duration of the experiment. The decrease of the operating voltages did not appear to have an effect on regime II: the overall operational stability of the device remained similar (Supporting Information S1: Figure S16). We also note that the ON current decrease in IDTBT EG-OFETs operating in regime I has different characteristics than the irreversible degradation caused when exceeding the stable operational window in P3HT EG-OFETs. Though both effects are likely to be of electrochemical origin, the stable operational window for P3HT EG-OFETs has been reported to be 0.6 V,¹⁶⁻¹⁸ which is a value for which regime I is suppressed for IDTBT EG-OFETs.

In regime II, the ON current slowly increases with time at the start of the experiment, which is attributed to the device charging, as the electrical double layers

gradually form. The current then reaches a steady state and remains stable for at least the duration of a 900-min overnight experiment. From day to day, the baseline decreases slowly when measured in the dark (i.e., using an enclosed setup) to avoid photo-oxidation (Supporting Information S1: Figure S17), as done typically with these polymers.²⁹ Nonpolarizable electrodes, such as Ag/AgCl, were not used for EG-OFET operational stability experiments, as they have demonstrated instabilities after prolonged operation (Supporting Information S1: Figure S18). Even though the operational stability was similar across all four electrolytes, the requirements to achieve stability for each electrolyte are different: Stability in ultrapure water can be achieved with clean fabrication protocols and avoiding the sources of contamination identified above. For stability in saline solution, corrosion-resistant (e.g., Ti/Pt/Au) source-drain contacts are also needed. Additionally, thiolation of the source-drain contacts with 3,3,4,4,5,5,6,6,7,7,8,8,8-tridecafluoro-1-octanethiol was found necessary to achieve stability in $1 \times$ PBS and NaP buffer (Supporting Information S1: Figure S19). The thiolated self-assembled monolayer (SAM) likely acts as a contact passivation layer. A similar passivating strategy on Au source-drain contacts has been shown to inhibit the reductive bias stress-driven reaction that accelerates degradation in thiophene-based OEFTs.⁵⁷ We also found that molecular additives can improve the water stability but only if they remain in the organic semiconductor. Since the additives are water soluble, they leave the film if the organic semiconductor is in direct contact with the electrolyte, as in the case of EG-OFETs (Supporting Information S1: Figures S20, S21). However, they can significantly improve the stability of OFETs if a hydrophobic dielectric layer is used to keep them in the film (Supporting Information S1: Figures S22, S23, S24).

Our optimized devices remain stable during an individual overnight experiment, with consecutive liquid injections not affecting the ON current's slope (drift) and magnitude. As shown in Supporting Information S1: Table S1, the median values of the ON current drift in the steady state are $\approx 0.2\%/h$ in ultrapure water, $\approx 0.1\%/h$ in $1 \times$ PBS, and $< 0.1\%/h$ in saline solution and NaP buffer. This is an order of magnitude improvement over the drift of P3HT EG-OFETs ($1\%/h$).¹⁴ The overall lifetime of our IDTBT EG-OFETs exceeds 2 months in ultrapure water and 1 month in the other electrolytes. The devices were not measured beyond these periods; so, their actual lifetime is likely to be larger. In contrast, P3HT EG-OFETs were reported to have a lifetime of 20 days.¹⁴ The operational stability and lifetime timescales of our optimized devices are the longest recorded so far in the literature. We emphasize that this is the first study

showcasing stable EG-OFETs, not just in ultrapure water but in a variety of other widely used electrolytes relevant to biosensing (saline solution, $1 \times$ PBS, NaP buffer).

Another important advantage of IDTBT EG-OFETs is that they are not affected by electrical stress-induced trap states, unlike P3HT EG-OFETs. As mentioned in the introduction, the ON current of P3HT EG-OFETs decreases linearly with the number of measurements.²⁹ Their drift is $1\%/h$ only if the interval between measurements is 30 min, and if this interval is reduced to 30 s, they are unable to reach a steady state. Our stability results were obtained by measuring one transfer curve per minute. This suggests that IDTBT EG-OFETs are likely not just one but several orders of magnitude more stable than P3HT EG-OFETs.

Our IDTBT EG-OFETs can even remain stable in operating voltages of -1 V, where electrochemical doping occurs. As seen in Supporting Information S1: Figure S13, some devices were electrochemically doped, as reflected in an increase of the OFF current. This is an important finding because until now the electrochemical doping of the organic semiconductor has been linked to EG-OFET degradation.^{17,18} As mentioned in the introduction, when P3HT EG-OFETs are measured above the stable operational window of 0.6 V,^{16–18} ions penetrate deeper in the organic semiconductor,^{19,20} causing electrochemical doping^{17,18} and irreversibly degrading the device. Even though our study shows that EG-OFET degradation and electrochemical doping are not necessarily related, we did empirically observe that unstable EG-OFETs have larger OFF currents than stable devices. Supporting Information S1: Figure S10 shows that devices made with Ti/Pt/Au contacts that are stable in saline solution have smaller OFF currents than devices made with Ti/Au contacts that corrode. Similarly, devices made with thiolated contacts that are stable in $1 \times$ PBS and NaP buffer have smaller OFF currents than devices made with nonthiolated contacts that degrade (Supporting Information S1: Figure S19E–H). Finally, devices made with a thicker Ti adhesion layer also have smaller OFF currents than devices made with a thinner Ti adhesion layer, which are generally more unstable (Supporting Information S1: Figure S11B).

Even though the baseline ON current of our optimized devices is orders of magnitude more stable than other devices reported in the literature, the ON current slowly decreases from day to day in regime II. The baseline drift between experiments averaged across the device lifetime is $< 1\%/day$ for ultrapure water and NaP buffer, $\approx 1.5\%/day$ for $1 \times$ PBS, and $\approx 2.5\%/day$ for saline solution. Since the transfer curves did not exhibit a clear threshold voltage shift toward more negative values (Supporting Information S1: Figure S14), the observed

decrease is attributed to a mobility reduction or a capacitance reduction.^{58,59} The origin of this is currently not well understood. It could be due to a slow contamination of the surface of the polymer reducing the double layer capacitance at the interface or a slow electrochemical degradation of the polymer due to reaction with residual reactive species present in the flow system or generated by the operation of the device, such as H_2O_2 .⁵⁷ The correlation between unstable performance in regime II and increased OFF currents suggests that the slow baseline decrease is most likely an electrochemical process associated with ion diffusion in the organic semiconductor. Because the choice of bottom contacts can lead to increased OFF currents and more unstable performance, we cannot safely attribute this degradation to electrochemical doping, which depends on the operating voltages and on the choice of electrolytes. Identification of this long-term degradation mechanism requires a careful analytical study that goes beyond the scope of the present work and will be undertaken in the next phase of this research.

Having optimized the stability of IDTBT EG-OFETs, we performed a long-term biosensing demonstration. We chose lysozyme as an analyte because it is a protein that is involved in many biological functions and can be detected through its net charge, without requiring gate functionalization.^{58,60} Figure 5 shows lysozyme sensing tests with our most optimized (fourth) generation of IDTBT EG-OFETs in ultrapure water and NaP buffer. The EG-OFETs were first measured until they were able to maintain a stable baseline overnight (i.e., until they reached regime II). Each liquid was injected four times, with the first four injections being those of the pure

electrolyte, followed by those of the lysozyme solutions with different concentrations. A total of 70 min of measurements were taken after each injection (1 transfer curve per minute), thus ensuring that the device was measured in the steady state.

The baseline remained stable during injections of the same solution but scaled with the lysozyme concentration in measurements lasting for 1500 min. The corresponding transfer curves at each protein concentration are shown in Supporting Information S1: Figure S25. The change of ON current from the baseline scales linearly (Supporting Information S1: Figure S26) with the lysozyme concentration in both electrolytes, with the ON current increasing in ultrapure water and decreasing in NaP buffer. The different ON current response suggests different sensing mechanisms in the two electrolytes. The increasing lysozyme concentrations cause a change in the ON current in ultrapure water and a threshold voltage shift in NaP buffer (Supporting Information S1: Figure S25). Therefore, a mobility or capacitance increase most likely happens in ultrapure water, while electrostatic charge sensing dominates in NaP buffer.^{58,59} Understanding the sensing mechanism will require detailed investigations of how the protein interacts with the surfaces of the device, which goes beyond the scope of the present work. Based on these sensing modalities, the limits of detection (LOD) and sensitivities (S) in NaP buffer and ultrapure water are calculated as $\text{LOD} = 28 \mu\text{g/mL}$, $S = 1.1 \times 10^{-6} \text{ A}/(\text{mg/mL})$ and $50 \mu\text{g/mL}$, $3.4 \times 10^{-6} \text{ A}/(\text{mg/mL})$, respectively. Even though previously reported P3HT EG-OFETs⁸ or other FET sensors⁶¹ have reported better performance, one should bear in mind that this proof of principle

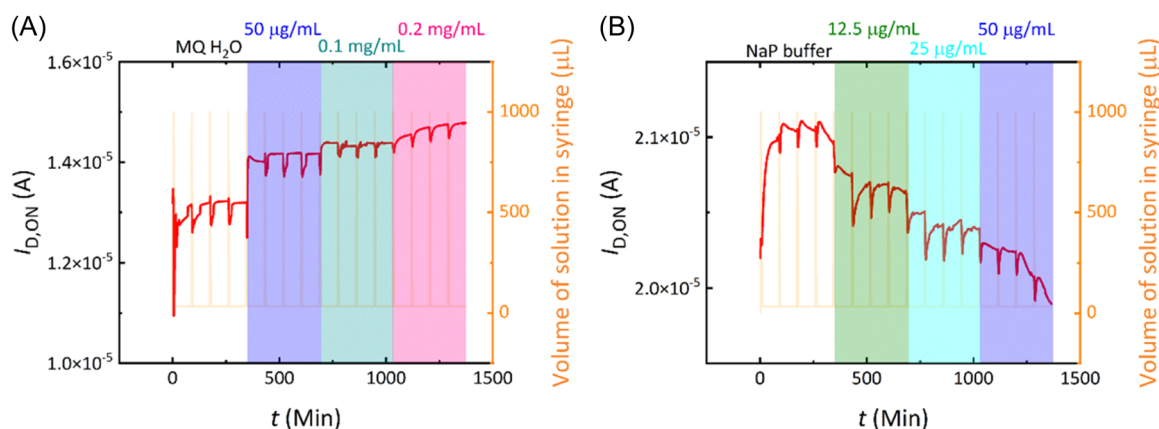


FIGURE 5 Lysozyme sensing tests with indacenodithiophene-co-benzothiadiazole (IDTBT) electrolyte-gated organic field-effect transistors (EG-OFETs) (A) in ultrapure water and (B) sodium phosphate (NaP) buffer in measurements lasting for 1500 min. The vertical triangular spikes correspond to the liquid injections (orange curve). Each liquid was injected four times. The EG-OFETs were able to sense lysozyme in both electrolytes, with the baseline remaining stable during injections of the same solution. The baseline scaled with the lysozyme concentration in both electrolytes, with the ON current increasing in ultrapure water and decreasing in NaP buffer.

experiment was not optimized for biosensing but rather to showcase the stability of our devices. Strategies to improve the biosensing performance include surface functionalization⁶² and transport optimization.⁵⁰

Increasing the lysozyme concentration beyond a certain limit caused an irreversible electrochemical reaction that led to a logarithmic response of the ON current (Supporting Information S1: Figure S27). The same reaction can also be observed after 1200 min in Figure 5B. In this regime, the device is unable to reach a steady state, and the ON current increases logarithmically with time, independently of the liquid injections. Hence, this regime cannot be used for biosensing, and once the device enters this regime, it cannot recover when injected with pure electrolyte. These irreversible electrochemical effects depend on the ionic strength of the electrolyte.^{63,64} When a more conductive electrolyte is used (e.g., NaP buffer), the electrochemical effects appear in smaller lysozyme concentrations. The same electrochemical effects appear when lysozyme accumulates in the device (Supporting Information S1: Figure S27B). Therefore, each sensing experiment was performed using a new EG-OFET. Still, these electrochemical phenomena introduce an additional sensing mode, a thresholding type of response that might be useful in detecting when the concentration exceeds a certain value.

4 | CONCLUSIONS

In this work, we demonstrated EG-OFET devices with ultrahigh operational stability and lifetime, suitable for long-term sensing applications in aqueous electrolytes. This was achieved using a systematic approach to eliminate multiple degradation factors. Among them, contaminants leaching from plastic laboratory consumables as well as residual un-crosslinked PDMS were shown to affect the stability of the EG-OFET baseline. Interestingly, the response from such contamination could easily be interpreted as a sensing event. We also identified galvanic corrosion as a major degradation mechanism, when the device is measured in conductive electrolytes, and mitigated it by using corrosion-resistant metal contacts. Importantly, we presented IDTBT EG-OFETs that can be operated continuously and remain operationally stable for an overnight experiment (≈ 900 min), in a variety of widely used electrolytes (ultrapure water, saline solution, $1 \times$ PBS, NaP buffer). Our devices have a median current drift of $\approx 0.2\%/h$ in ultrapure water, $\approx 0.1\%/h$ in $1 \times$ PBS, and $< 0.1\%/h$ in saline solution and NaP buffer, while being continuously measured. The overall device lifetime exceeds 2 months in ultrapure water and 1 month in the other electrolytes. These operational stability and lifetime timescales are the

longest recorded so far in the literature. The devices were not affected by electrical stress-induced trap states and can remain stable even in voltage ranges where electrochemical doping occurs. The stabilized EG-OFETs are able to sense lysozyme in ultrapure water and NaP buffer without gate functionalization. The baseline remained stable during injections of the same solution but scaled with the lysozyme concentration in measurements lasting for 1500 min. Our study demonstrates that organic semiconductors can be operationally stable in aqueous electrolytes and that polymer-based EG-OFETs are a viable architecture for short- and long-term biosensing applications. It also provides insight into the stability-limiting mechanisms that might allow further optimization of the operational stability of EG-OFETs. The strategies of controlling contamination and corrosion should also improve the operational stability of other organic electronic devices that are operated in direct contact with aqueous electrolytes, such as OECTs.

ACKNOWLEDGMENTS

D.S., M.N., and J.C. contributed equally to this work. The authors acknowledge funding from the Engineering and Physical Sciences Research Council (EPSRC) (Nos. EP/R031894/1, EP/R032025/1, EP/W017091/1). D.S. acknowledges support from the EPSRC Centre for Doctoral Training (CDT) in Sensor Technologies and Applications (No. EP/L015889/1), as well as advice from Prof. Luisa Torsi that steered the project in the right direction. M.N. acknowledges funding from the European Commission under a global Marie-Curie fellowship. Z.T. acknowledges funding from the Ron Thomson Research Fellowship, Pembroke College. I.E.J. acknowledges funding from a Royal Society Newton International Fellowship. I.B.D. acknowledges support from the EPSRC Cambridge NanoDTC (No. EP/L015978/1). G.S. thanks the Belgian National Fund for Scientific Research (FNRS) for financial support through research project COHERENCE2 No. F.4536.23. G.S. is an FNRS Research Associate. G.S. acknowledges financial support from the Francqui Foundation (Francqui Start-Up Grant). H.S. thanks the Royal Society for a Royal Society Research Professorship (No. RP/R1/201082). The authors acknowledge support by the Henry Royce Institute facilities grant (No. EP/P024947/1), as well as the Henry Royce Institute recurrent grant (No. EP/R00661X/1) for use of the ambient cluster tool and the Cambridge XPS System.

CONFLICT OF INTEREST STATEMENT

H.S. is the Chief Scientist of FlexEnable Ltd. Professor Henning Sirringhaus is the Associate Editor of the journal. However, he was excluded from the peer-review process and all editorial decisions related to the

publication of the article entitled “Electrolyte-gated organic field-effect transistors with high operational stability and lifetime in practical electrolytes.”

DATA AVAILABILITY STATEMENT

The data that support the findings of this study are available online, from the Apollo repository (DOI: [10.17863/CAM.106919](https://doi.org/10.17863/CAM.106919)).⁶⁵

ORCID

Dimitrios Simatos  <https://orcid.org/0000-0003-0300-9249>

Mark Nikolka  <https://orcid.org/0000-0002-3556-1970>

Jérôme Charmet  <http://orcid.org/0000-0001-6992-4090>

Leszek J. Spalek  <https://orcid.org/0000-0001-5154-5690>

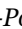
Zenon Toprakcioglu  <https://orcid.org/0000-0003-1964-8432>

Ian E. Jacobs  <https://orcid.org/0000-0002-1535-4608>

Ivan B. Dimov  <https://orcid.org/0000-0003-3513-583X>

Guillaume Schweicher  <https://orcid.org/0000-0002-6501-0790>

Mi Jung Lee  <https://orcid.org/0000-0002-9677-5788>

Carmen M. Fernández-Posada  <https://orcid.org/0000-0003-3080-1637>

Duncan J. Howe  <https://orcid.org/0000-0001-7549-236X>

Tuuli A. Hakala  <https://orcid.org/0000-0002-2075-3451>

Vincenzo Pecunia  <https://orcid.org/0000-0003-3244-1620>

Maryam Alsufyani  <https://orcid.org/0000-0003-4097-7900>

Iain McCulloch  <https://orcid.org/0000-0002-6340-7217>

Tuomas P. J. Knowles  <https://orcid.org/0000-0002-7879-0140>

Henning Sirringhaus  <http://orcid.org/0000-0001-9827-6061>

REFERENCES

- Kergoat L, Herlogsson L, Braga D, et al. A water-gate organic field-effect transistor. *Adv Mater.* 2010;22(23):2565-2569.
- Cramer T, Campana A, Leonardi F, et al. Water-gated organic field effect transistors -opportunities for biochemical sensing and extracellular signal transduction. *J. Mater. Chem. B.* 2013;1(31):3728-3741.
- Herlogsson L, Crispin X, Robinson ND, et al. Low-voltage polymer field-effect transistors gated via a proton conductor. *Adv Mater.* 2007;19(1):97-101.
- Bhalla N, Jolly P, Formisano N, Estrela P. Introduction to biosensors. *Essays Biochem.* 2016;60(1):1-8.
- Clarke GA, Hartse BX, Niaraki Asli AE, et al. Advancement of sensor integrated organ-on-chip devices. *Sensors.* 2021;21(4):1367.
- Fuchs S, Johansson S, Tjell AØ, Werr G, Mayr T, Tenje M. In-line analysis of organ-on-chip systems with sensors: integration, fabrication, challenges, and potential. *ACS Biomater Sci Eng.* 2021;7(7):2926-2948.
- Zhu Y, Mandal K, Hernandez AL, et al. State of the art in integrated biosensors for organ-on-a-chip applications. *Curr. Opin. Biomed. Eng.* 2021;19:100309.
- Macchia E, Manoli K, Holzer B, et al. Single-molecule detection with a millimetre-sized transistor. *Nat Commun.* 2018;9(1):3223.
- Nikolka M. A perspective on overcoming water-related stability challenges in molecular and hybrid semiconductors. *MRS Commun.* 2020;10(1):98-111.
- Knopfmacher O, Hammock ML, Appleton AL, et al. Highly stable organic polymer field-effect transistor sensor for selective detection in the marine environment. *Nat Commun.* 2014;5(1):2954.
- Torricelli F, Adrahtas DZ, Bao Z, et al. Electrolyte-gated transistors for enhanced performance bioelectronics. *Nat. Rev. Methods Primers.* 2021;1(1):66.
- Zhang Q, Leonardi F, Casalini S, Temiño I, Mas-Torrent M. High performing solution-coated electrolyte-gated organic field-effect transistors for aqueous media operation. *Sci Rep.* 2016;6(1):39623.
- Wang D, Noël V, Piro B. Electrolytic gated organic field-effect transistors for application in biosensors—a review. *Electronics.* 2016;5(1):9.
- Picca RA, Manoli K, Macchia E, et al. A study on the stability of water-gated organic field-effect-transistors based on a commercial p-type polymer. *Front Chem.* 2019;7:667.
- Nikolka M, Nasrallah I, Rose B, et al. High operational and environmental stability of high-mobility conjugated polymer field-effect transistors through the use of molecular additives. *Nat Mater.* 2017;16(3):356-362.
- Schmoltner K. *Environmentally stable organic field-effect transistor based sensor devices.* Doctor of Philosophy. Graz University of Technology; 2014.
- Schmoltner K, Kofler J, Klug A, List-Kratochvil EJW. Electrolyte-gated organic field-effect transistors for sensing in aqueous media. In: SPIE Proceedings, San Diego, United States, 18th September 2013. International Society for Optics and Photonics; 2013.
- Kofler J, Schmoltner K, Klug A, List-Kratochvil EJW. Hydrogen ion-selective electrolyte-gated organic field-effect transistor for pH sensing. *Appl Phys Lett.* 2014;104(19):193305.
- Thomas EM, Brady MA, Nakayama H, Popere BC, Segalman RA, Chabinyc ML. X-ray scattering reveals ion-induced microstructural changes during electrochemical gating of poly(3-Hexylthiophene). *Adv Funct Mater.* 2018;28(44):1803687.
- Guardado JO, Salleo A. Structural effects of gating poly(3-hexylthiophene) through an ionic liquid. *Adv Funct Mater.* 2017;27(32):1701791.
- Robinson L, Isaksson J, Robinson ND, Berggren M. Electrochemical control of surface wettability of poly(3-alkylthiophenes). *Surf Sci.* 2006;600(11):L148-L152.
- Robinson L, Hentzell A, Robinson ND, Isaksson J, Berggren M. Electrochemical wettability switches gate

- aqueous liquids in microfluidic systems. *Lab Chip*. 2006; 6(10):1277-1278.
23. Laiho A, Herlogsson L, Forchheimer R, Crispin X, Berggren M. Controlling the dimensionality of charge transport in organic thin-film transistors. *Proc Natl Acad Sci*. 2011;108(37):15069-15073.
 24. Larsson O, Laiho A, Schmickler W, Berggren M, Crispin X. Controlling the dimensionality of charge transport in an organic electrochemical transistor by capacitive coupling. *Adv Mater*. 2011;23(41):4764-4769.
 25. de Leeuw DM, Simenon MMJ, Brown AR, Einerhand REF. Stability of n-type doped conducting polymers and consequences for polymeric microelectronic devices. *Synth Met*. 1997;87(1):53-59.
 26. Porrazzo R, Bellani S, Luzio A, Lanzarini E, Caironi M, Antognazza MR. Improving mobility and electrochemical stability of a water-gated polymer field-effect transistor. *Org Electron*. 2014;15(9):2126-2134.
 27. Rainbolt JE, Koech PK, Polikarpov E, et al. Synthesis and characterization of p-type conductivity dopant 2-(3-(adamantan-1-yl)propyl)-3,5,6-trifluoro-7,7,8,8-tetracyanoquin odimethane. *J Mater Chem C*. 2013;1(9):1876-1884.
 28. Mello HJNPD, Dalgleish S, Ligorio G, Mulato M, List-Kratochvil EJW. Stability evaluation and gate-distance effects on electrolyte-gated organic field-effect transistor based on organic semiconductors. In: SPIE Proceedings, San Diego, United States, 10th October 2018. International Society for Optics and Photonics; 2018.
 29. Luukkonen A, Tewari A, Björkström K, et al. Long-term electrical characteristics of a poly-3-hexylthiophene water-gated thin-film transistor. *Org Electron*. 2023;120:106844.
 30. Wuytens R, Santermans S, Gupta M, et al. Two-regime drift in electrolytically gated FETs and bioFETs. In: 2020 IEEE International Reliability Physics Symposium (IRPS). IEEE; 2020:1-5.
 31. Zhang W, Smith J, Watkins SE, et al. Indacenodithiophene semiconducting polymers for high-performance, air-stable transistors. *J Am Chem Soc*. 2010;132(33):11437-11439.
 32. McCulloch I, Ashraf RS, Biniek L, et al. Design of semiconducting indacenodithiophene polymers for high performance transistors and solar cells. *Acc Chem Res*. 2012;45(5):714-722.
 33. Venkateshvaran D, Nikolka M, Sadhanala A, et al. Approaching disorder-free transport in high-mobility conjugated polymers. *Nature*. 2014;515(7527):384-388.
 34. Bronstein H, Leem DS, Hamilton R, et al. Indaceno dithiophene-co-benzothiadiazole copolymers for high performance solar cells or transistors via alkyl chain optimization. *Macromolecules*. 2011;44(17):6649-6652.
 35. Doumbia A, Tong J, Wilson RJ, Turner ML. Investigation of the performance of donor-acceptor conjugated polymers in electrolyte-gated organic field-effect transistors. *Adv Electron Mater*. 2021;7(9):2100071.
 36. Vasilescu A, Wang Q, Li M, Boukherroub R, Szunerits S. Aptamer-based electrochemical sensing of lysozyme. *Chemosensors*. 2016;4(2):10.
 37. Ohring M, Kasprzak L. *Reliability and Failure of Electronic Materials and Devices*. 2nd ed. Elsevier/Academic Press; 2015.
 38. English AT, Turner PA. Stability of conductor metallizations in corrosive environments. *J Electron Mater*. 1972;1(1):1-15.
 39. Holloway PH. Gold/chromium metallizations for electronic devices. *Gold Bull*. 1979;12(3):99-106.
 40. Simatos D, Jacobs IE, Dobryden I, et al. Effects of processing-induced contamination on organic electronic devices. *Small Methods*. 2023;7(11):2300476.
 41. Yumusak C, Sariciftci NS, Irimia-Vladu M. Purity of organic semiconductors as a key factor for the performance of organic electronic devices. *Mater Chem Front*. 2020;4(12):3678-3689.
 42. Griggs S, Marks A, Meli D, et al. The effect of residual palladium on the performance of organic electrochemical transistors. *Nat Commun*. 2022;13(1):7964.
 43. Nikiforov MP, Lai B, Chen W, et al. Detection and role of trace impurities in high-performance organic solar cells. *Energy Environ Sci*. 2013;6(5):1513-1520.
 44. Jacobs IE, Wang F, Bedolla Valdez ZI, Ayala Oviedo AN, Bilsky DJ, Moulé AJ. Photoinduced degradation from trace 1,8-diiodooctane in organic photovoltaics. *J Mater Chem C*. 2018;6(2):219-225.
 45. Chang L, Jacobs IE, Augustine MP, Moulé AJ. Correlating dilute solvent interactions to morphology and OPV device performance. *Org Electron*. 2013;14(10):2431-2443.
 46. McDonald GR, Hudson AL, Dunn SMJ, et al. Bioactive contaminants leach from disposable laboratory plasticware. *Science*. 2008;322(5903):917.
 47. Jug U, Naumoska K, Metličar V, et al. Interference of oleamide with analytical and bioassay results. *Sci Rep*. 2020;10(1):2163.
 48. Olivieri A, Degenhardt OS, McDonald GR, et al. On the disruption of biochemical and biological assays by chemicals leaching from disposable laboratory plasticware. *Can J Physiol Pharmacol*. 2012;90(6):697-703.
 49. Pereira I, Fomitcheva Khartchenko A, Petrini L, Kaigala GV. Nip the bubble in the bud: a guide to avoid gas nucleation in microfluidics. *Lab Chip*. 2019;19(14):2296-2314.
 50. Squires TM, Messinger RJ, Manalis SR. Making it stick: convection, reaction and diffusion in surface-based biosensors. *Nat Biotechnol*. 2008;26(4):417-426.
 51. Tahvildari R, Beamish E, Briggs K, et al. Manipulating electrical and fluidic access in integrated nanopore-microfluidic arrays using microvalves. *Small*. 2017;13(10):1602601.
 52. Revie RW, ed. *Uhlig's Corrosion Handbook*. 3rd ed. Wiley; 2011.
 53. Baghalha M. Leaching of an oxide gold ore with chloride/hypochlorite solutions. *Int J Miner Process*. 2007;82(4):178-186.
 54. Anderson JC. Applications of thin films in microelectronics. *Thin Solid Films*. 1972;12(1):1-15.
 55. Nowicki RS, Nicolet MA. General aspects of barrier layers for very-large-scale integration applications II: practice. *Thin Solid Films*. 1982;96(4):317-326.
 56. Todeschini M, Bastos da Silva Fanta A, Jensen F, Wagner JB, Han A. Influence of Ti and Cr adhesion layers on ultrathin Au films. *ACS Appl Mater Interfaces*. 2017;9(42):37374-37385.
 57. Schafer EA, Wu R, Meli D, et al. Sources and mechanism of degradation in p-type thiophene-based organic electrochemical transistors. *ACS Appl Electron Mater*. 2022;4(4):1391-1404.
 58. Manoli K, Magliulo M, Mulla MY, et al. Printable bioelectronics to investigate functional biological interfaces. *Angew Chem Int Ed*. 2015;54(43):12562-12576.

59. Heller I, Janssens AM, Männik J, Minot ED, Lemay SG, Dekker C. Identifying the mechanism of biosensing with carbon nanotube transistors. *Nano Lett.* 2008;8(2):591-595.
60. Steudle A, Pleiss J. Modelling of lysozyme binding to a cation exchange surface at atomic detail: the role of flexibility. *Biophys J.* 2011;100(12):3016-3024.
61. Syu YC, Hsu WE, Lin CT. Review—field-effect transistor biosensing: devices and clinical applications. *ECS J Solid State Sci Technol.* 2018;7(7):Q3196-Q3207.
62. Macchia E, Tiwari A, Manoli K, et al. Label-free and selective single-molecule bioelectronic sensing with a millimeter-wide self-assembled monolayer of anti-immunoglobulins. *Chem Mater.* 2019;31(17):6476-6483.
63. Höger K, Mathes J, Frieß W. IgG1 adsorption to siliconized glass vials—influence of pH, ionic strength, and nonionic surfactants. *J Pharm Sci.* 2015;104(1):34-43.
64. Lee SH, Ruckenstein E. Adsorption of proteins onto polymeric surfaces of different hydrophilicities—a case study with bovine serum albumin. *J Colloid Interface Sci.* 1988;125(2):365-379.
65. Siringhaus H, Simatos D, Nikolka M, et al. Research data supporting: “Electrolyte-gated organic field-effect transistors with high operational stability and lifetime in practical electrolytes”. Apollo - University of Cambridge Repository; 2024. <https://doi.org/10.17863/CAM.106919>

SUPPORTING INFORMATION

Additional supporting information can be found online in the Supporting Information section at the end of this article.

How to cite this article: Simatos D, Nikolka M, Charmet J, et al. Electrolyte-gated organic field-effect transistors with high operational stability and lifetime in practical electrolytes. *SmartMat.* 2024;e1291. [doi:10.1002/smm2.1291](https://doi.org/10.1002/smm2.1291)